Triterpenoids from *Alisma orientale* and their NF-κB Inhibitory Activity

Authors
Qian Yang[1, 4], Yinqing Li[2, 3], Xizi Liu[1, 4], Shiyi Han[1, 4], Siyang Fan[1, 4]

Affiliations
1 State Key Lab. of New Drug and Pharmaceutical Process, China State Institute of Pharmaceutical Industry, Shanghai, PR China
2 Shineway Pharmaceutical Group Ltd., Shijiazhuang, PR China
3 Hebei key Laboratory of Famous Classical Formulas and TCM Quality Process Control, Shijiazhuang, PR China
4 Innovation center of Traditional Chinese Medicine, Shanghai Institute of Pharmaceutical Industry, Shanghai, PR China

Key words
Alisma orientale, Alismataceae, triterpenoids, nuclear factor-kappa B

received 10.03.2021
revised 23.06.2021
accepted 25.06.2021

Bibliography
Planta Med Int Open 2021; 8: e114–e121
DOI 10.1055/a-1543-1261
ISSN 2509-9264

Georg Thieme Verlag KG, Rüdigerstraße 14,
70469 Stuttgart, Germany

Correspondence
Dr. Siyang Fan
State Key Lab. of New Drug and Pharmaceutical Process
China State Institute of Pharmaceutical Industry, Innovation center of Traditional Chinese Medicine, Shanghai Institute of Pharmaceutical Industry
285 Gebaini Road
Shanghai
P. R. China
Tel: +86-21-20572000-2047, Fax: 02162474199
max_121@163.com

Supplementary Material is availale under https://doi.org/10.1055/a-1543-1261.

ABSTRACT

The rhizome of *Alisma orientale* (sam.) Juz. is used in clinics for eliminating dampness, reducing edema, and promoting diuresis. This study aimed to elucidate the compounds and investigate their nuclear factor-kappa inhibitory activities in human embryonic kidney 293 cells. A new triterpene, alismaketone B (**1**); a new natural nortriterpene, noralisolic acid A (**2**); and 13 known protostane-type triterpenes were isolated from the rhizome of *A. orientale*. The new structures and their absolute configurations were established using HRESIMS, NMR, and electronic circular dichroism experiments. All isolated compounds were evaluated for their inhibitory activity on NF-κB. The compounds **8, 9, 10,** and **14** showed moderate NF-κB inhibitory activities with their IC_{50} values being 64.7, 32.3, 47.3, and 37.3 μM, respectively.

ABBREVIATIONS

TCM	traditional Chinese medicine
NF-κB	nuclear factor-kappa B
ECD	electronic circular dichroism
TDDFT	time-dependent density functional theory
CC	column chromatography

Introduction

Alisma orientale (Sam.) Juz. (Alismataceae) is an aquatic medicinal herb mainly harvested in Fujian, Jiangxi, and Sichuan, China. This plant's dried tubers (Rhizoma alismatis), known as "Zexie" in China [1], are often used in clinics for eliminating dampness, reducing edema, and promoting diuresis [2, 3]. Triterpenes [4, 5] and sesquiterpenes [6] are the major components in *A. orientale* tubes. Pharmacological studies showed that this plant's ethanol or water extracts have diuretic [7], lipid-lowering [8], liver-protecting [9],

hypoglycemic [10], anti-inflammatory [11], and renal protective activities [12]. Besides, *A. orientale*'s ethanol extract attenuates lung inflammation in LPS-induced acute lung injury mice by suppressing NF-κB and nuclear factor erythroid-2 related factor 2 activities [13, 14]. However, the *A. orientale*'s triterpenoids' inhibitory activities on NF-κB are still to be studied.

In this study, 15 protostane-type triterpenoids (**1–15**), including a new triterpenoid, alismaketone B **(1),** and a new natural nortriterpene, noralisolic acid A **(2)**, as well as a known fatty acid compound (**16**), were identified from *A. orientale*'s rhizomes (▶ **Fig. 1**). The new compounds' absolute structures were elucidated by various spectroscopic or spectrometric methods, including 1D and 2D NMR, HRESIMS, and ECD. HEK293/NF-κB cells were used to investigate the 15 triterpenoids' NF-κB inhibition potential, and the isolates' IC_{50} values were evaluated for their activities. These compounds exhibited NF-κB inhibition properties and could explain the plant's traditional use to treat renal diseases.

Results and Discussion

The rhizomes of *A. orientale* were extracted with 60 % EtOH to produce a brown crude extract. The extract was separated using silica gel and ODS-A column chromatography as well as semi-preparative HPLC into a new triterpenoid (**1**), alismaketone B; a new natural nortriterpene, noralisolic acid A (**2**); and 14 known compounds (**3–16**). Compound identification was performed using mass spectrometry and NMR spectroscopy, and spectroscopic data were compared with reference compounds reported in the literature. The known compounds were identified as follows: alisol C 23-acetate (**3**) [15], alisol Q 23-acetate (**4**) [15], 16,23-oxido-alisol B (**5**) [16], alismalactone 23-acetate (**6**) [17], alisol A (**7**) [15], 25-*O*-methylalisol A (**8**) [18], alisol B (**9**) [15], 25-*O*-ethylalisol A (**10**) [18], alisol C (**11**) [16], alisol F (**12**) [19], 16-oxo-11-deoxy-alisol A (**13**) [16], alisol A 24-acetate (**14**) [15], 16-oxoalisol A (**15**) [16], and (9*Z*,12*Z*)-2,3-dihydroxypropyl octadecadienoate (**16**) [20].

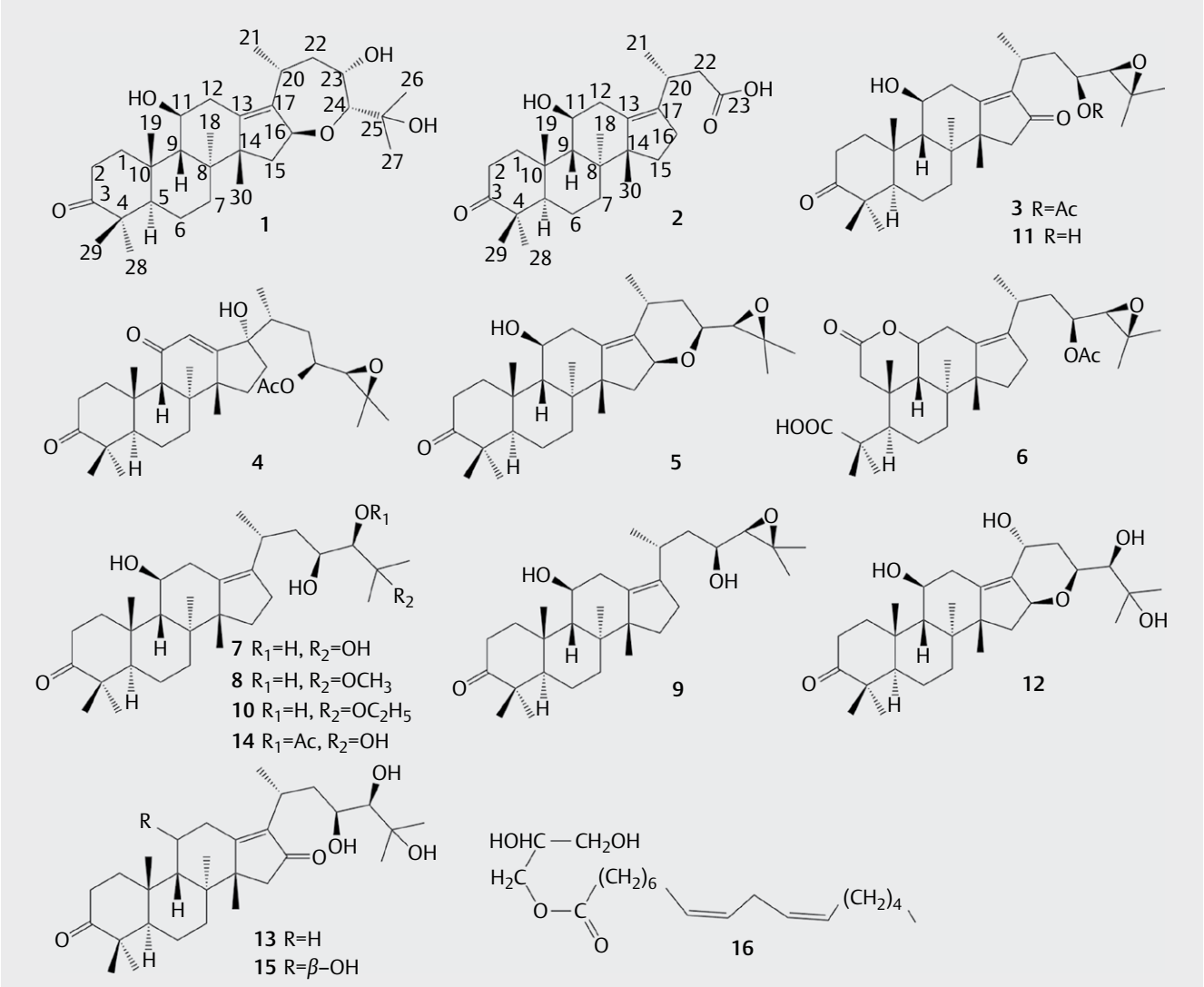

▶ **Fig. 1** Compounds isolated from *A. orientale*.

Compound **1** was obtained as a yellow amorphous powder. This compound's molecular formula was established as $C_{30}H_{48}O_5$ with a positive HRESIMS (*m/z* 533.3499, calcd. 533.3478, $[M+HCOO]^-$). The ^1H NMR spectrum (▶ **Table 1**) of **1** showed the presence of 8 methyl groups at δ_H 1.32 (s), 1.27 (s), 1.19 (s), 1.17 (d, *J* = 7.1 Hz), 1.07 (s), 1.06 (s), 1.05 (s), and 0.89 (s) and 4 oxygenated methines at δ_H 5.13 (t, *J* = 6.5 Hz), 4.10 (m), 3.28 (m), and 3.83 (m). The ^{13}C NMR spectrum displayed 30 signals, including a carbonyl carbon at δ_C 220.0; 2 olefinic carbons at δ_C 142.6 and 135.5; 4 oxygenated methine carbons at δ_C 69.9, 71.7, 76.6, and 83.6; and an oxygenated quaternary carbon at δ_C 73.7. Furthermore, 4 quaternary carbons, 3 methines, 7 methylenes, and 8 methyls were determined using ^{13}C NMR and DEPT experiments. These data closely resembled those of alismaketones B 23-acetate [21], except for the absence of an acetyl group at C-23. Accordingly, compound **1** should have a hydroxyl group at C-23 instead of the 23-acetate of alismaketones B 23-acetate. The structure of compound **1** was confirmed by the correlations of H-26 (δ_H 1.32)/C-27 (δ_C 28.6), H-24 (δ_H 3.28)/C-27 (δ_C 28.6), H-23 (δ_H 4.10)/C-20(δ_C 28.7), H-21(δ_H 1.17)/C-22(δ_C 41.2), and H-16 (δ_H 5.13)/C-24 (δ_C 76.6) observed in the HMBC spectrum, which we have shown in ▶ **Fig. 2**.

▶ **Table 1** ^1H (400 MHz) and ^{13}C (100 MHz) NMR for compounds **1** and **2** in $CDCl_3$.

Pos.	1		2	
	δ_H, *J* (Hz)	δ_C	δ_H, *J* (Hz)	δ_C
1	2.20 m	30.7 (t)	2.23 m	31.0 (t)
	2.06 m		2.10 m	
2	2.67 m	33.5 (t)	2.66 m	33.7 (t)
	2.34 m		2.33 m	
3	–	220.0 (s)	–	220.4 (s)
4	–	46.9 (s)	–	47.0 (s)
5	2.11 m	48.2 (d)	2.08 m	48.5 (d)
6	1.47 m	19.9 (t)	1.45 m	20.0 (t)
	1.28 m		1.29 m	
7	2.02 m	34.4 (t)	2.70 m	34.3 (t)
	1.28 m		1.23 m	
8	–	40.6 (s)	–	40.5 (s)
9	1.75 d (10.7)	49.3 (d)	1.72 d (10.6)	49.6 (d)
10	–	36.9 (s)	–	36.9 (s)
11	3.83 m	69.9 (d)	3.85 m	70.0 (d)
12	2.64 m	34.1 (t)	2.76 m	34.4 (t)
	2.08 m		2.02 m	
13	–	142.6 (s)	–	137.3 (s)
14	–	54.8 (s)	–	57.0 (s)
15	2.32 m	40.0 (t)	1.87 m	30.5 (t)
	1.33 m		1.34 m	
16	5.13 t (6.5)	83.8 (d)	2.29 m	29.3 (t)
			2.17 m	
17	–	135.6 (s)	–	134.5 (s)
18	1.19 s	23.6 (q)	0.97 s	24.1 (q)
19	1.06 s	25.4 (q)	1.05 s	25.6 (q)
20	2.69 m	28.7 (d)	3.07 m	29.4 (d)
21	1.17 d (7.1)	20.8 (q)	1.06 d (7.1)	19.5 (q)
22	1.88 m	41.2 (t)	2.31 m	40.0 (t)
	1.70 m			
23	4.10 m	71.7 (d)	–	177.0 (s)
24	3.28 m	76.6 (d)	–	–
25	–	73.7 (s)	–	–
26	1.32 s	26.1 (q)	–	–
27	1.27 s	28.6 (q)	–	–
28	1.07 s	29.5 (q)	1.07 s	29.6 (q)
29	1.05 s	20.0 (q)	1.05 s	20.1 (q)
30	0.89 s	23.5 (q)	1.10 s	22.8 (q)

The relative configuration of compound **1** was established from the $^3J_{H,H}$ coupling value as well as NOESY data. A considerable $^3J_{9,11}$ value of 10.7 Hz indicated the axial-axial relationship of H-9 and H-11. As shown in ▶ **Fig. 2**, the NOESY correlations of Me-18 (δ_H 0.89) with H-5 (δ_H 2.11), H-11 (δ_H 3.83), H-16 (δ_H 5.13), and H-15α (δ_H 2.32); the correlations of Me-30 (δ_H 1.19) with H-9 (δ_H 1.75) and H-24 (δ_H 3.28); and the correlation of H-24 (δ_H 3.28) with H-15β (δ_H 1.33) indicated that H-5, H-11, H-16, and Me-18 were α-oriented, whereas H-9, H-24, and Me-30 were β-oriented. Additionally, the correlations of Me-19 (δ_H 1.06)/H-9 (δ_H 1.75), H-20 (δ_H 2.70)/H-23 (δ_H 4.10), H-11(δ_H 3.83)/Me-21 (δ_H 1.17), and H-16 (δ_H 5.13)/Me-21 (δ_H 1.17) indicated the β-configurations of Me-19, H-20, and H-23. Compound **1**'s experimental ECD spectrum showed a positive cotton effect at 290 nm and a negative cotton effect at 205 nm. The comparison between the TDDFT calculated spectrum (B3LYP/6-311 G * level) and the experimental data showed good agreement with 5*R*, 8*R*, 9*S*, 10*S*, 11*S*, 14*S*, 15*S*, 20*R*, 23*S*, and 24*R*. Still, the alternative form revealed a curve with the opposite cotton effect (▶ **Fig. 3**). To the best of our knowledge, **1** was designated as the new protostane-type triterpenoid alismaketone B.

Compound **2** was obtained as a yellow amorphous powder. This compound's molecular formula was assigned as $C_{26}H_{40}O_4$ by negative HRESIMS at *m/z* 461.2883 $[M+HCOO]^-$ (calcd. 461.2903). The ^1H-NMR spectrum (▶ **Table 1**) showed 6 tertiary methyl groups at δ_H 0.97 (s), 1.05 (s), 1.05 (s), 1.06 (d, *J* = 7.1 Hz), 1.07 (s), and 1.10 (s) and an oxygenated proton signal at δ_H 3.85 (1H, m). The ^{13}C-NMR data displayed signals for 2 carbonyls at δ_C 220.4 and 177.0. Compound **2**'s ^1H and ^{13}C NMR spectroscopic data were highly similar to those reported for alisol A (**7**) [15], except for the absence of oxygenated carbon signals at C-23, C-24, and C-25, and the presence of an additional carbonyl group (δ_C 177.0). Accordingly, **2** should have a carboxyl group at C-23 instead of the triol unit of alisol A (**7**). This feature is consistent with HMBC correlations observed (▶ **Fig. 4**) between H-22 (δ_H 2.31) and C-23 (δ_C 177.0), C-21 (δ_C 40.0) and C-17 (δ_C 134.5), H-20 (δ_H 3.07) and C-23 (δ_C 177.0), as well as between H-20 (δ_H 3.07) and C-16 (δ_C 29.3).

A considerable $^3J_{9,11}$ value of 10.6 Hz indicated the axial-axial relationship of H-9 and H-11. The NOESY correlations of Me-18 (δ_H 0.97)/H-11 (δ_H 3.85), H-11/H-5 (δ_H 2.08), Me-18/H-15α (δ_H 1.87), Me-30 (δ_H 1.10)/H-9 (δ_H 1.72), Me-30/H-15β (δ_H 1.34), and H-9/Me-19 (δ_H 1.05) supported the chair, boat, and chair conformations of rings A, B, and C, as well as their ring junction's *trans-cis-trans* relationships (▶ **Fig. 4**). The experimental ECD spectrum of **2** showed a positive cotton effect at 293 nm and a negative cotton effect at 203 nm. A comparison of the TDDFT-calculated spectrum (B3LYP/6–

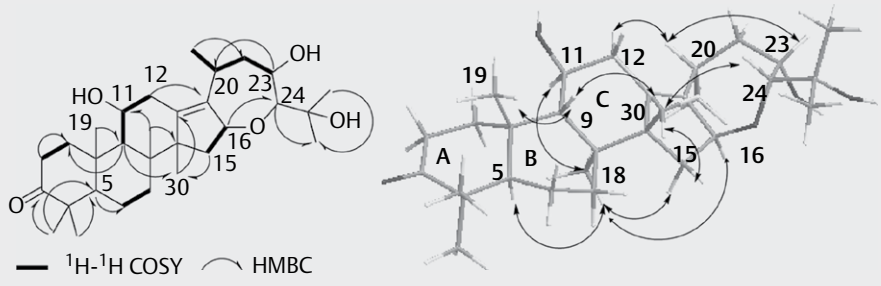

▶ **Fig. 2** Key ^{1}H-^{1}H COSY, HMBC (H→C) and NOESY (↔) correlations of compound **1.**

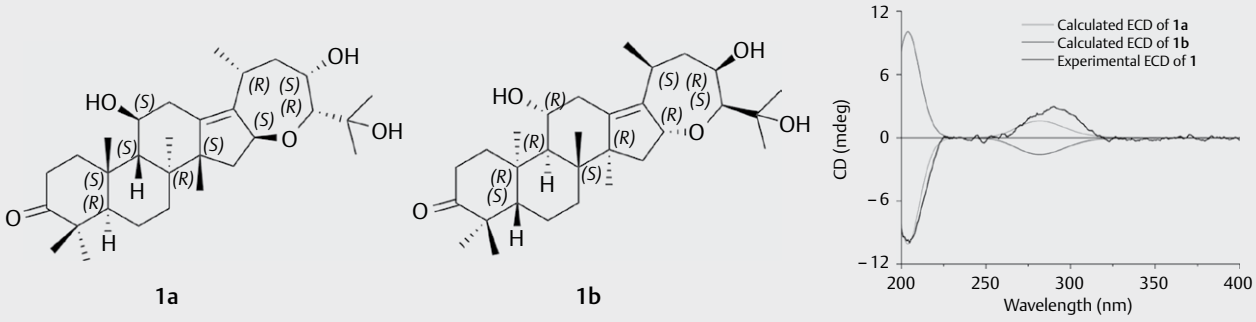

▶ **Fig. 3** Experimental and calculated ECD spectra of **1** in MeOH.

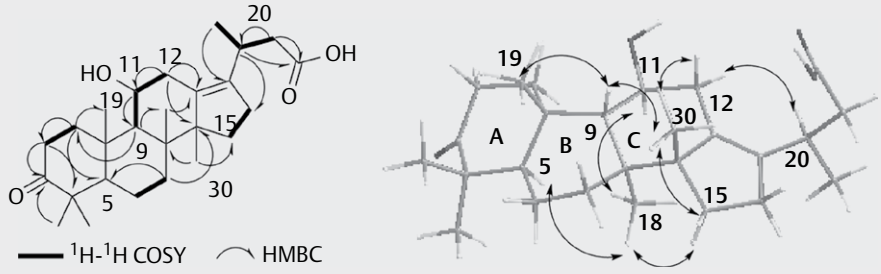

▶ **Fig. 4** Key ^{1}H-^{1}H COSY, HMBC (H→C) and NOESY (↔) correlations of compound **2.**

311 G * level) and the experimental data showed good agreement with 5*R*, 8*R*, 9*S*, 10*S*, 11*S,* and 14*S*, while the alternative form revealed a curve with the opposite cotton effect (▶**Fig. 5**). Besides, the absolute configuration at C-20 was considered to be *R* based on the biogenesis of the protostane skeleton [22]. For the first time, the absolute configuration of **2** was discussed. Compound **2** was assigned as a new natural nortriterpenoid noralisolic acid A.

Lee reported the synthesis of noralisolic acid A, and its structure was assigned based on IR analysis and limited NMR data [23]. The ^{13}C-NMR data of synthetic noralisolic acid A closely resembled those of compound **2,** except for the lower field shift of the signal of C-22 (δ_C 57.7). However, this assignment of C-22's chemical shift was considered incorrect based on the following evidence: (1) the methylene carbon attached to the carboxyl group may give a signal at approximately δ_C 38.0 [24]; (2) an HMBC correlation from H-22 (δ_H 2.31) to C-23 (δ_C 177.0) permitted the carboxyl group of compound **2** to be attached to C-22.

Compounds **1**–**15** were evaluated for their NF-κB inhibition activity in TNF-α stimulated HEK 293 cell line. Triterpenoids **8**–**10** and **14** showed moderate inhibitory activity with IC_{50} values of 64.7, 32.3, 47.3, and 37.3 μM, respectively. However, the other compounds displayed mild NF-κB inhibition at a maximum tested concentration of 50 μM. Additionally, the IC_{50} of IMD-0354 was 13.3 μM, which was proved that the test system and calculation method were feasible. The results were shown in ▶**Table 2** and ▶**Fig. 6**. The results indicated that the sp^3 hybrid C-16 of Alisma

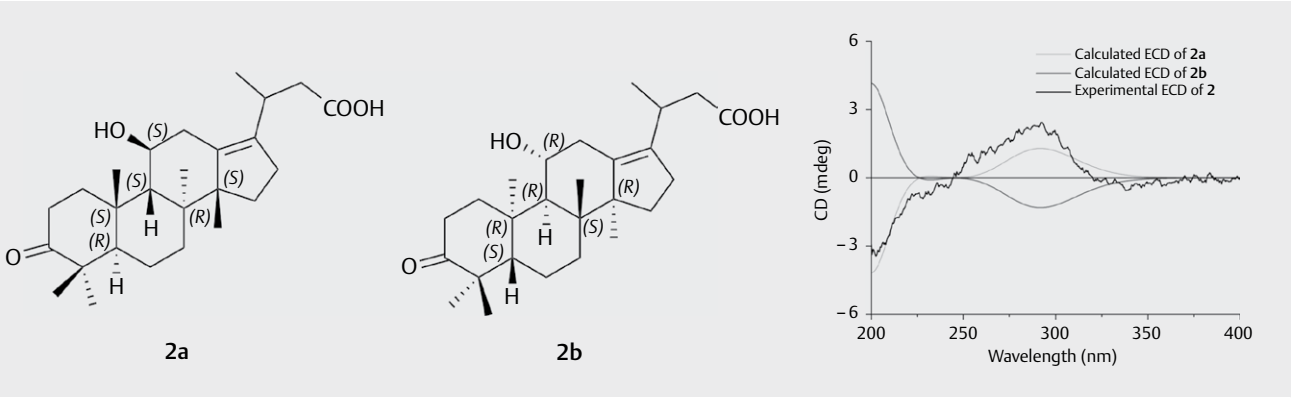

▶ **Fig. 5** Experimental and calculated ECD spectra of compound **2** in MeOH.

▶ **Table 2** NF-κB cell line HEK293 inhibitory activities of active compounds.

compound	inhibition rate (%)	IC_{50} (μM)
8	58.4 ± 0.0[a]	64.7 (C.I. 33.4–139.2)
9	94.8 ± 0.4[a]	47.3 (C.I. 29.2–78.3)
10	51.7 ± 3.7[a]	47.3 (C.I. 29.2–78.3)
14	64.8 ± 3.8[a]	37.3 (C.I. 24.3–59.5)
IMD0354	57.6 ± 2.7[b]	13.3 (C.I. 10.2–17.6)

[a] Measured in 50 μM; [b] Measured in 30 μM. IC_{50} was afforded with confidence interval (n = 2); C.I.: 95 % confidence interval. Positive control: IMD-0354.

triterpenoids (**8–10** *vs.***3, 11, 13,** and **15**) is essential for NF-κB inhibition. The side-chain cyclization at C-17 depleted the NF-κB inhibition (**9** *vs.***5**). The hydroxyl groups at C-23 and the less hydrophilic groups at C-24/25 (-OAc or epoxy group) contributed to the NF-κB inhibitory activity (**9** and **14** *vs.***3**, **4**, **6**, **8**, **10**, **13,** and **15**) (▶ **Fig. 7**).

It has been reported that ethanol extract of *A. orientale* tuber could suppress LPS-induced NF-κB activity and NF-κB dependent gene expression in RAW 264.7 cells. Alisol B (**9**) was detected in EEAO by HPLC analysis but was not tested for its NF-κB inhibitory activity [13]. Our results confirmed that not only alisol B (**9**) but also 25-*O*-methylalisol A (**8**), 25-*O*-ethylalisol A (**10**), and alisol A 24-acetate (**14**) were involved in NF-κB activity. Compounds **9** and **14** were also reported to show anti-inflammatory and anti-allergic activities *via* inhibiting CD147 and MMP-9 secretion and leukotriene production [25–27].

In addition, compounds **1–15** were also tested for their antihuman dihydroorotate dehydrogenase activity by the reported method [28]. Nonetheless, they did not show any benefit (Data not shown).

Materials and Methods

General experimental procedures

IR spectra were recorded on Chiral IR-2X vibrational circular dichroism spectrometer in deuterated chloroform. The optical rotation was determined on JASCO P-2000 automatic polarimeter in MeOH. NMR spectra were measured on Bruker Avance DRX-400. HRESIMS was performed on Waters Xevo G2-XS Q-TOF mass spectrometer, and the semi-preparative HPLC was performed on Chuangxin Tongheng 3050 N HPLC system with a C_{18} column (YMC-Pack ODS-A, 5 μm, 10.0 × 250 mm). The ECD spectra were acquired in MeOH using JASCO J-815 circular dichroism spectrometer. Chemiluminescence measurements for the NF-κB cell line HEK293 inhibition assay were recorded on Envision (PerkinElmer).

Solvents and chemicals

IMD-0354 (purity ≥ 99 %) was purchased from Aladdin. DMEM was acquired from BI and FBS from Gibco. Penicillin and streptomycin (P/S) were obtained from Procell. Bright–Glo was gifted by Promega. TNF-α was purchased from Peprotech. DMSO was acquired from Sigma. The solvents used for extraction and chromatographic separation were of analytical purity.

Plant material

The rhizomes of *A. orientale* were sampled from Pengshan County, Sichuan Province in China, in November 2018 and authenticated by Prof. Tong Wu from Pharmacognosy Department. A voucher specimen (20190409) was deposited in the Shanghai Institute of Pharmaceutical Industry.

Extraction and isolation

The air-dried and powdered rhizomes (5.0 kg) of *A. orientale* were extracted with 60 % EtOH (15 L × 3) for 3 times (2 h each time) under reflux. The combined solution was concentrated to crudeness *in vacuo*, and the crude extract was suspended in water (3 L), sequentially partitioning it with petroleum ether (60–90 °C) and dichloromethane (3 × 3 L each), respectively. The dichloromethane extract (120.4 g) was chromatographed on a silica gel column (CC) (6 × 72 cm; 200–300 mesh) and eluted by petroleum ether/ethyl acetate (50:1, 20:1, 10:1, 4:1, 2:1,1:1, v/v) to give 8 fractions (Fr.1–8) based on TLC analyses. Fr.4 (11.17 g) was subjected to an ODS-A gel CC (6.6 × 20 cm; S-50 μm,12 nm; YMC) and eluted by MeOH/H_2O (1:9, 3:7, 1:1, 7:3, 9:1, and 1:0 v/v) to yield 9 fractions (Fr.4a–4i). Fr.4b (1.73 g) was purified using semi-preparative HPLC (60 % CH_3CN in water; 4.0 mL/min; UV detection at λ 210 nm) to isolate

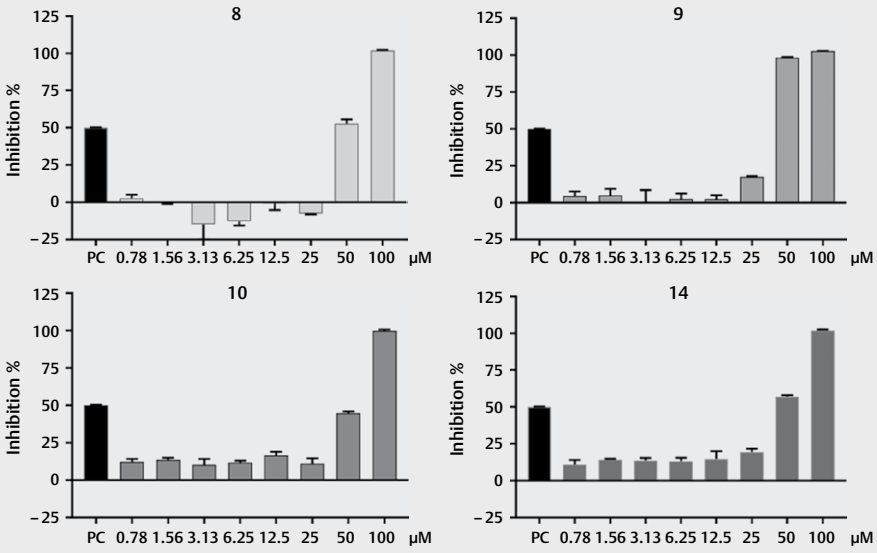

▶ **Fig. 6** Inhibitory activity of compounds **8**, **9**, **10,** and **14** in TNF-α stimulated HEK293 cells. HEK293 cells were treated with indicated doses of constituents for 24 h, and then chemiluminescence was determined. IMD-0354 was used as a positive control and possessed an inhibitory rate of approximately 50 % at 15 μM. Experiments were performed in duplicate, and data were represented as means ± SD.

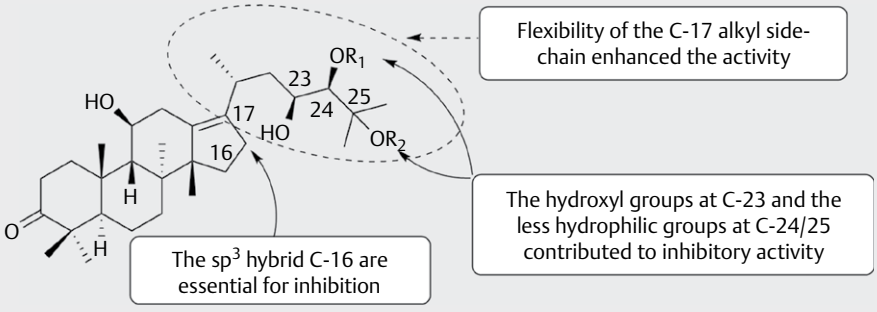

▶ **Fig. 7** Protostane-type triterpenoids' structure-activity relationships.

compound **3** (326.0 mg, t_R = 21 min). Fr.4d (0.79 g) was purified *via* semi-preparative HPLC (50 % CH_3CN in water; 4.0 mL/min; UV detection at λ 210 nm) to afford compounds **4** (16.5 mg, t_R = 37 min) and **5** (10.2 mg, t_R = 42 min). Compounds **6** (62.4 mg, t_R = 65.2 min) and **2** (22.9 mg, t_R = 27.9 min; 97 % purity by HPLC) were obtained from Fr.4 f (0.44 g) through semi-preparative HPLC eluted using CH_3CN/H_2O (78:22, v/v; 3.0 mL/min; UV detection at λ 210 nm). Fr.4 h (2.96 g) was subjected to semi-preparative HPLC with CH_3CN/H_2O (60:40–80:20, v/v, 90 min; 4.0 mL/min; UV detection at λ 210 nm) to obtain compounds **7–10** (62.5, 85.8, 228.5, and 34.5 mg, respectively; t_R = 14.7, 28.2, 31.6, and 41.2 min). Compound **16** (17.3 mg, t_R = 21.3 min) was purified from Fr.4i (0.32 g) by semi-preparative HPLC (80 % CH_3CN in water; 4.0 mL/min; UV detection at λ 210 nm). Fr.6 (6.45 g) was subjected to an ODS-A gel CC eluted with $MeOH/H_2O$ (1:9, 3:7, 1:1, 7:3, 9:1, and 1:0, v/v) to obtain 6 fractions (Fr.6a–6 f). Fr.6b (1.17 g) was further purified *via* semi-preparative HPLC (40 % CH_3CN in water; 3.0 mL/min; UV detection at λ 210 nm) to obtain compounds **11**, **12**, **13** (150.0, 30.0, and 26.0 mg, t_R = 24, 56 and 31 min) and **1** (16.1 mg, t_R = 33 min; 93 % purity by HPLC). Compound **14** (12.1 mg, t_R = 29 min) was obtained from Fr.6d (0.37 g) and purified using semi-preparative HPLC eluted with CH_3CN/H_2O (57:43, v/v; 3.0 mL/min; UV detection at λ 210 nm). Finally, Fr.6e (0.25 g) was subjected to semi-preparative HPLC with CH_3CN/H_2O (35:65, v/v; 3.0 mL/min; UV detection at λ 210 nm) to obtain compound **15** (40.1 mg, t_R = 21.1 min).

Alismaketone B (1): yellow amorphous powder; $[\alpha]_D^{24}$ + 53.4 (c 0.02, MeOH); ECD (MeOH) λ_{max} (Δε) 290 (+ 2.98), 205 (− 9.96); IR ($CDCl_3$) V_{max} 3390, 2941, 1695 cm^{-1}; ^1H and ^{13}C NMR spectroscopic data (see ▶ **Tables 1**); HRESIMS at *m/z* 533.3499 $[M + HCOO]^-$ (calcd. for $C_{31}H_{49}O_7$, 533.3478).

Noralisolic acid A (2): yellow amorphous powder; $[\alpha]_D^{24}$ + 57.0 (c 0.04, MeOH); ECD (MeOH) λ_{max} (Δε) 293 (+ 2.44), 203 (− 3.43); IR ($CDCl_3$) V_{max} 3444, 2941, 1747, 1699, 1654 cm^{-1}; ^1H and ^{13}C NMR spectroscopic data (see ▶ **Tables 1**); HRESIMS at *m/z* 415.2817

$[M-H]^-$, 831.5751 $[2M-H]^-$, 461.2883 $[M+HCOO]^-$ (calcd. for $C_{27}H_{41}O_6$, 461.2903).

ECD calculation

Computational calculations were performed using the Gaussian 09 software. Conformers were generated by the MMFF94 force field and were obtained at 6 kcal/mol. Conformational analyses and geometry optimizations were performed at the B3LYP/6–311 G * level in MeOH. ECD calculations were performed by TDDFT at the B3LYP/6–311 G * level in MeOH. ECD spectra were obtained by weighing each geometric conformation's Boltzmann distribution rate with a bandwidth σ of 0.3 eV (**1**) or 0.4 eV (**2**).

Inhibitory effects on NF-κB cell line HEK293

The NF-κB activity in the TNF-α stimulated HEK293 cell line was used to evaluate the inhibitory effects of all these isolates using the modified Bright-Glo method [29]. Compounds **1–15** were dissolved in DMSO to prepare a stock solution, and then each stock solution was serially diluted 2-fold to different concentrations using a culture medium. HEK293 cells were cultured in a DMEM medium plus 10 % FBS and 1 % P/S were seeded in 96-well plates at a density of 40,000 cells/well with 80 µL. After incubating at 37 °C under 5 % CO_2 overnight, the tested compounds (10 µL) were added to the wells. They were incubated at the same conditions for 2 h, and TNF-α (10 µL, 20 ng/mL) was then added to each well and incubated in the darkness for 24 h. Chemiluminescence was measured on Envision after the addition of 50 µL Bright-Glo Luciferase Assay Reagent to each well.

$$\text{Inhibition}\,(\%) = 100 - (B/A \times 100)$$

Where, B was the luminescence value of tested compounds, and A was luminescence of the negative control group (with cells, medium, DMSO, and TNF-α).

Data were analyzed by GraphPad Prism v.7.0 and were presented as a geometric means with 95 % confidence intervals of 2 independent experiments. IMD-0354 was used as a positive control and DMSO as a negative control.

Supporting Information

The 1D/2D NMR and HREIMS spectra of compounds **1** and **2,** their optimized geometries, compounds **1** and **2'**s calculated conformers' ECD spectra, the triterpenoid's NF-κB cell line HEK293 inhibitory activities, as well as the compounds **3–16** experimental NMR data, are available as Supporting Information.

Acknowledgments

This work was supported by grants from the National Natural Science Foundation of China (No. 81603279), the National Science and Technology Project of China (No. 2018ZX09731–016), and the S&T Program of Hebei (20272502D). The authors would like to thank Professor Li in the Institute of Materia Medica, Chinese Academy of Medical Sciences, and Peking Union Medical College, for her help in ECD calculation.

Conflicts of interest

The authors declare that they have no conflict of interest.

References

[1] Pharmacopoeia CoN. Pharmacopoeia of the People's Republic of China. Beijing: The Medicine Science and Technology Press of China; 2020

[2] Shu Z, Pu J, Chen L, Zhang Y, Rahman K, Qin L, Zheng C. *Alisma orientale*: Ethnopharmacology, phytochemistry and pharmacology of an important traditional Chinese medicine. Am J Chin Med 2016; 44: 227–251

[3] Zhang LL, Xu W, Xu YL, Chen X, Huang M, Lu JJ. Therapeutic potential of *Rhizoma Alismatis*: a review on ethnomedicinal application, phytochemistry, pharmacology, and toxicology. Ann N Y Acad Sci 2017; 1401: 90–101

[4] Li HM, Chen XJ, Luo D, Fan M, Zhang ZJ, Peng LY, Wu XD, Li RT, Ji X, Zhao Q-S. Protostane-type triterpenoids from *Alisma orientale*. Chem Biodivers 2017; 14: e1700452

[5] Xin XL, Xin XL, Zhao XY, Huo XK, Sun CP, Zhang HL, Tian Y, Zhao XY, Liu Y, Tian X-G, Wang X. Two new protostane-type triterpenoids from *Alisma orientalis*. Nat Prod Res 2018; 32: 189–194

[6] Li HM, Fan M, Xue Y, Peng LY, Wu XD, Liu D, Li RT, Zhao QS. Guaiane-type sesquiterpenoids from *Alismatis rhizoma* and their anti-inflammatory activity. Chem Pharm Bull 2017; 65: 403–407

[7] Feng YL, Chen H, Tian T, Chen DQ, Zhao YY, Lin RC. Diuretic and anti-diuretic activities of the ethanol and aqueous extracts of *Alismatis rhizoma*. J Ethnopharmacol 2014; 154: 386–390

[8] Xu F, Yu H, Lu C, Chen J, Gu W. The cholesterol-lowering effect of alisol acetates based on HMG-CoA reductase and its molecular mechanism. Evid Based Complement Alternat Med 2016; 2016: 4753852

[9] Huo XK, Liu J, Yu ZL, Wang YF, Wang C, Tian XG, Ning J, Feng L, Sun CP, Zhang BJ, Ma XC. *Alisma orientale* extract exerts the reversing cholestasis effect by activation of farnesoid X receptor. Phytomedicine 2018; 42: 34–42

[10] Lin HR. Triterpenes from *Alisma orientalis* act as farnesoid X receptor agonists. Bioorg Med Chem Lett 2012; 22: 4787–4792

[11] Zhao XY, Wang G, Wang Y, Tian XG, Zhao JC, Huo XK, Sun CP, Feng L, Ning J, Wang C, Zhang B-J, Wang X. Chemical constituents from *Alisma plantago-aquatica* subsp. orientale (Sam.) Sam and their anti-inflammatory and antioxidant activities. Nat Prod Res 2018; 32: 2749–2755

[12] Dou F, Miao H, Wang JW, Chen L, Wang M, Chen H, Wen AD, Zhao YY. An integrated lipidomics and phenotype study reveals protective effect and biochemical mechanism of traditionally used *Alisma orientale* juzepzuk in chronic kidney disease. Front Pharmacol 2018; 9: 53

[13] Han CW, Kwun MJ, Kim KH, Choi JY, Oh SR, Ahn KS, Lee JH, Joo M. Ethanol extract of *Alismatis rhizoma* reduces acute lung inflammation by suppressing NF-κB and activating Nrf2. J Ethnopharmacol 2013; 146: 402–410

[14] Kim KH, Kwun MJ, Choi JY, Ahn KS, Oh SR, Lee YG, Christman JW, Sadikot RT, Han CW, Joo M. Therapeutic effect of the tuber of *Alisma orientale* on lipopolysaccharide-induced acute lung injury. Evid Based Complement Alternat Med 2013; 2013: 863892

[15] Jin H-G, Jin Q, Ryun Kim A, Choi H, Lee JH, Kim YS, Lee DG, Woo ER. A new triterpenoid from *Alisma orientale* and their antibacterial effect. Arch Pharmacal Res 2012; 35: 1919–1926

[16] Nakajima Y, Satoh Y, Katsumata M, Tsujiyama K, Ida Y, Shoji J. Terpenoids of *Alisma orientale* rhizomes and the crude drug *Alismatis rhizoma*. Phytochemistry 1994; 36: 119–127

[17] Yoshikawa M, Murakami T, Ikebata A, Ishikado A, Murakami N, Yamahara J, Matsuda H. Absolute stereostructures of alismalactone 23-acetate and alismaketone-a 23-acetate, new seco-protostane and protostane-type triterpenes with vasorelaxant effects from Chinese *Alismatis rhizoma*. Chem Pharm Bull 1997; 45: 756–758

[18] Mai ZP, Wang C, Huo XK, Dong PP, Deng S, Zhang BJ, Zhang HL, Huang SS, Ma XC, Zhou K, Ge GB. Protostane triterpenoids from the rhizome of *Alisma orientale* exhibit inhibitory effects on human carboxylesterase 2. J Nat Prod 2015; 78: 2372–2380

[19] Hu XY, Guo YQ, Gao WY, Zhang TJ, Chen HX. Two new triterpenes from the rhizomes of *Alisma orientalis*. J Asian Nat Prod Res 2008; 10: 487–490

[20] Lainer J, Dawid C, Dunkel A, Gläser P, Wittl S, Hofmann T. Characterization of bitter-tasting oxylipins in poppy seeds (Papaver somniferum L.). J Agr and Food Chem 2020; 68: 10361–10373

[21] Matsuda H, Kageura T, Toguchida I, Murakami T, Kishi A, Yoshikawa M. Effects of sesquiterpenes and triterpenes from the rhizome of *Alisma orientale* on nitric oxide production in lipopolysaccharide-activated macrophages: absolute stereostructures of alismaketones-B 23-acetate and-C 23-acetate. Bioorg Med Chem Lett 1999; 9(21): 3081–3086

[22] Zhao M, Gödecke T, Gunn J, Anh Tuan L, Che C-T. Protostane and fusidane triterpenes: A mini-review. Molecules 2013; 18: 4054–4080

[23] Lee SM, Min BS, Bae KH. Chemical modification of alisol B 23-acetate and their cytotoxic activity. Arch Pharm Res 2002; 25: 608–612

[24] Ma Q, Han L, Bi X, Wang X, Mu Y, Guan P, Li L, Huang X. Structures and biological activities of the triterpenoids and sesquiterpenoids from *Alisma orientale*. Phytochemistry 2016; 131: 150–157

[25] Kubo M, Matsuda H, Tomohiro N, Yoshikawa M. Studies on Alismatis Rhizoma. I. Anti-allergic effects of methanol extract and six terpene components from *Alismatis rhizoma* (dried rhizome of *Alisma orientale*). Biol Pharm Bull 1997; 20: 511–516

[26] Lee JH, Kwon OS, Jin HG, Woo ER, Kim YS, Kim HP. The rhizomes of *Alisma orientale* and alisol derivatives inhibit allergic response and experimental atopic dermatitis. Biol Pharm Bull 2012; 35: 1581–1587

[27] Shi FF, Wei W, Wang YC, Su QP, Xue XH. The effect of alisol A 24-acetate on lipid metabolic factors ABCA1, CD36 and inflammatory factors CD147, MMP-9 in oxidized low density lipoprotein-induced macrophages. Chin J Arteriosclerosis 2016; 24: 7–12

[28] Yang Q, Jia A, Liu XZ, Han SY, Fan SY. Chemical constituents from *Chloranthus elatior* and their inhibitory effect onhuman dihydroorotate dehydrogenase. Planta Med advance online publication 2021; doi: 10.1055/a-1449-2642

[29] Hino K, Nagata H, Shimonishi M, Ido M. High-throughput screening for small-molecule adiponectin secretion modulators. J Biomol Screen 2011; 16: 628–636